9.

Welding Defects

Figures 9.1 to 9.4 give a rough survey about the classification of welding defects to DIN 8524. This standard does not classify existing welding defects according to their origin but only to their appearance.

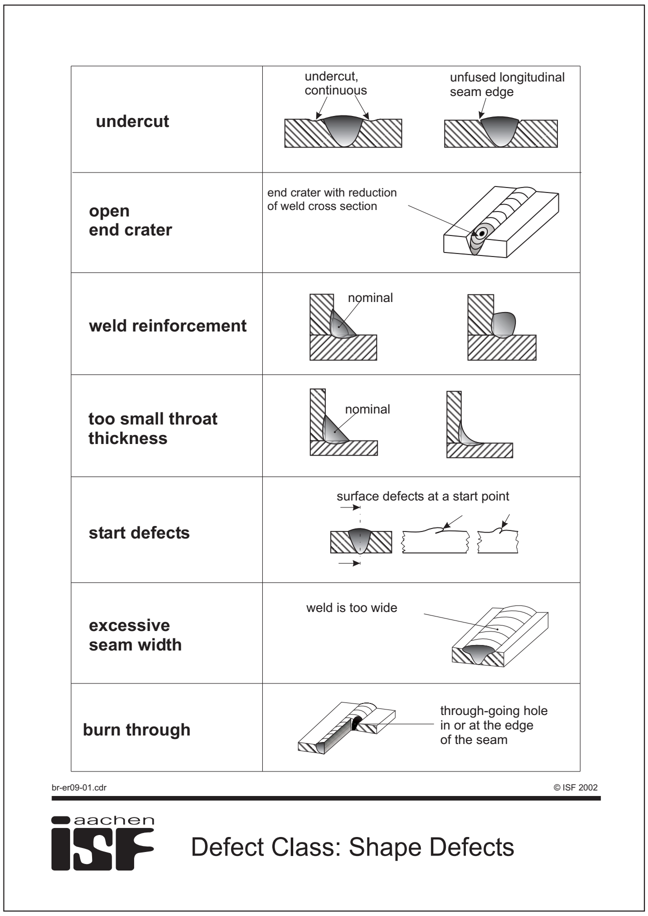

Figure 9.1

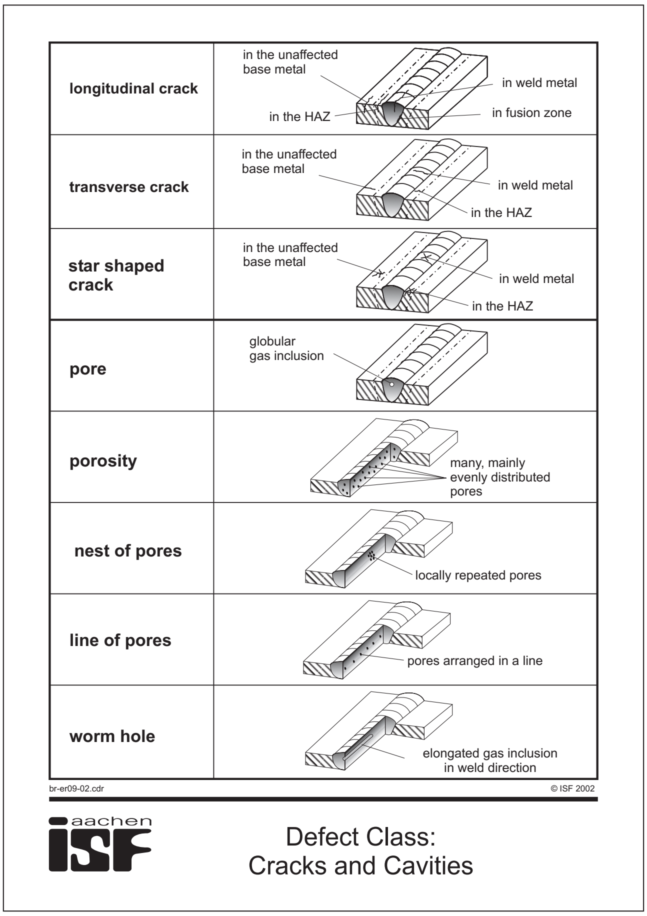

Figure 9.2

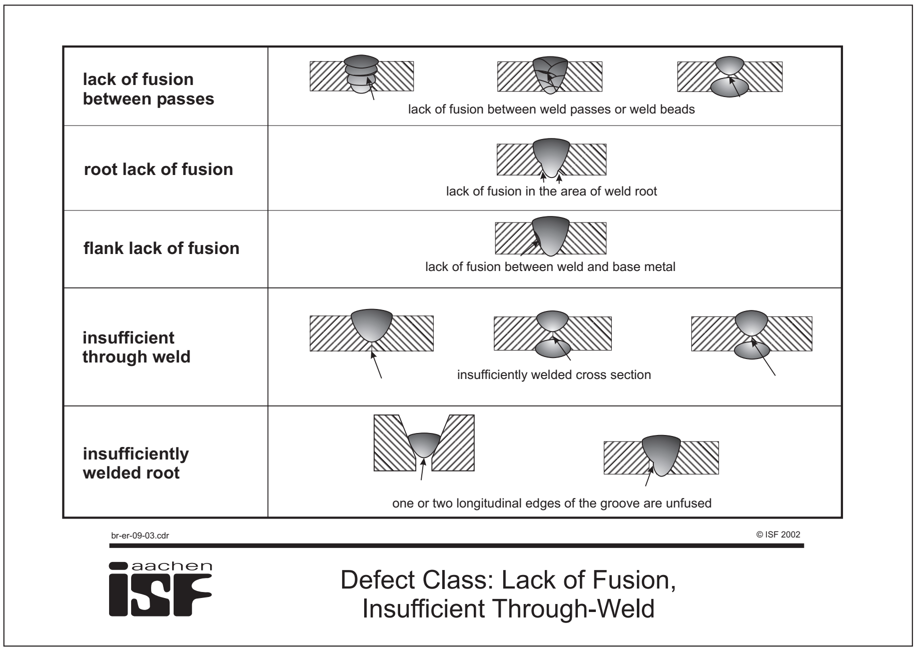

Figure 9.3

A distinction of arising defects by their origin is shown in Figure 9.5. The development of the most important welding defects is explained in the following paragraphs.

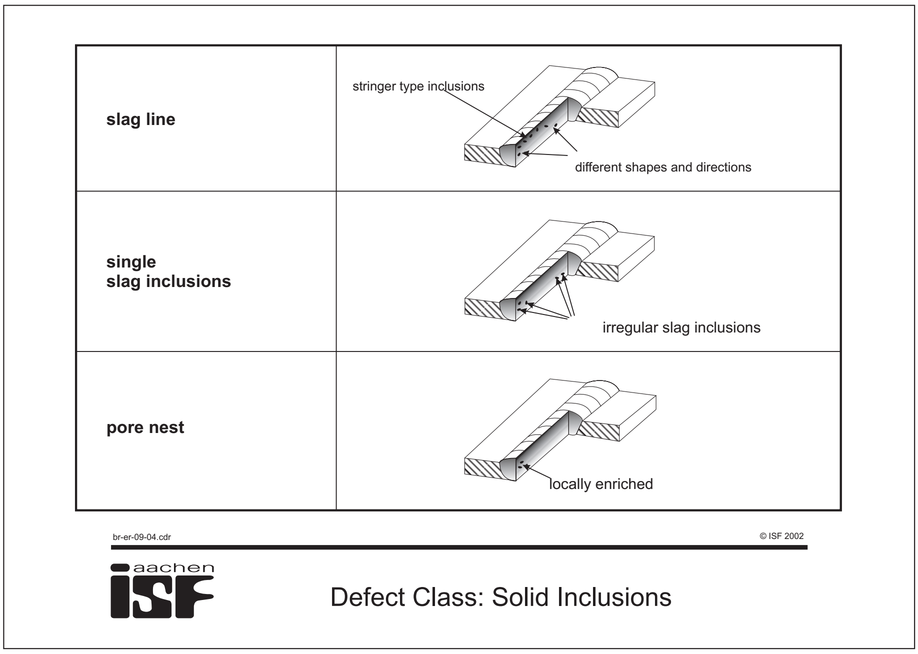

Figure 9.4

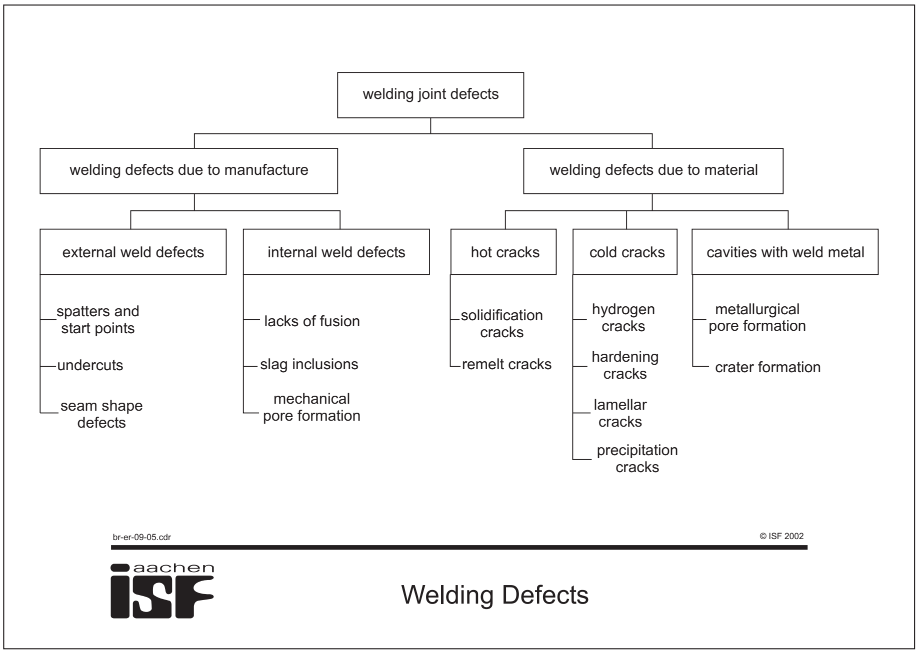

Figure 9.5

Lack of fusion is defined as unfused area between weld metal and base material or previously welded layer. This happens when the base metal or the previous layer are not completely or insufficiently molten. Figure 9.6 explains the influence of welding parameters on the development of lack of fusion. In the upper part, arc characteristic lines of MAG welding are shown using CO_2 and mixed gas. The welding voltage depends on welding current and is selected according to the joint type. With present tension, the welding current is fixed by the wire feed speed (thus also melting rate) as shown in the middle part of the figure.

Melting rate (resulting from selected welding parameters) and welding speed define the heat input. As it can be changed within certain limits, melting rate and welding speed do not limit each other, but a working range is created (lower part of the figure). If the heat input is too low, i.e. too high welding speed, a definite melting of flanks cannot be ensured. Due to the poor power, lack of fusion is the result. With too high heat input, i.e. too low welding speed, the weld pool gets too large and starts to flow away in the area in front of the arc. This effect prevents a melting of the base metal. The arc is not directed into the base metal, but onto the weld pool, and flanks are not entirely molten. Thus lack of fusion may occur in such areas.

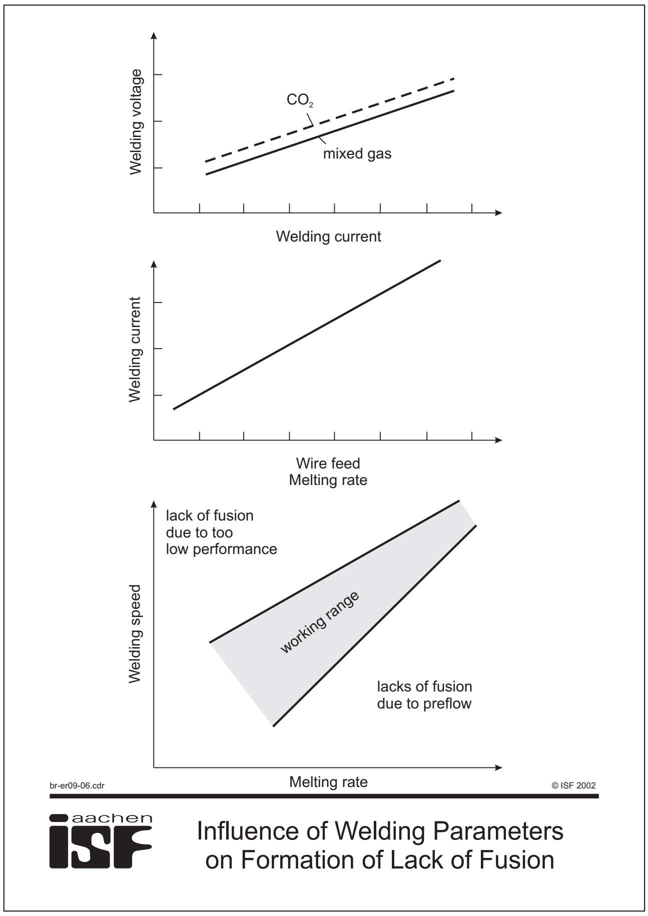

Figure 9.6

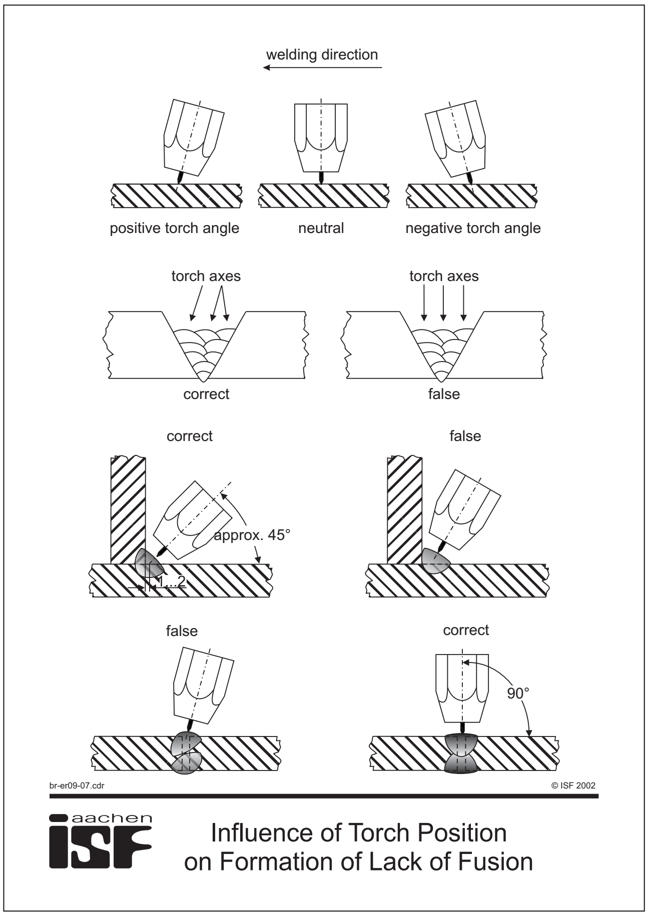

Figure 9.7

Figure 9.7 shows the influence of torch position on the development of weak fusion. The upper part of the figure explains the terms neutral, positive and negative torch angle. Compared with a neutral position, the seam gets wider with a positive inclination together with a slight reduction of penetration depth. A negative inclination leads to narrower beads. The second part of the figure shows the torch orientation transverse to welding direction with multi-pass welding. To avoid weak fusion between layers, the torch orientation is of great importance, as it provides a reliable melting and a proper fusion of the layers. The third figure illustrates the influence of torch orientation during welding of a fillet weld.

With a false torch orientation, the perpendicular flank is insufficiently molten, a lack of fusion occurs. When welding an I-groove in two layers, it must be ensured that the plate is completely fused. A false torch orientation may lead to lack of fusion between the layers, as shown in the lower figure.

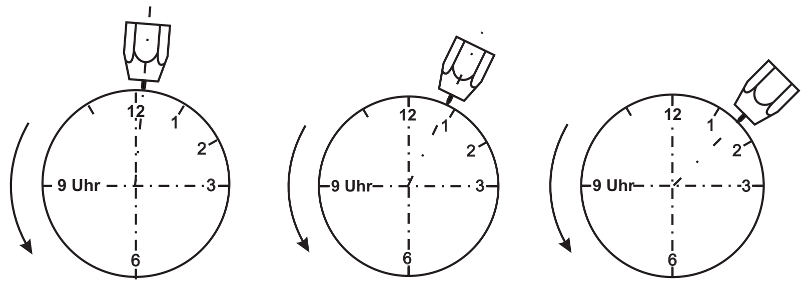

Influence of Torch Position
on Formation of Lacks of Fusion

Figure 9.8

Figure 9.8 shows the influence of the torch orientation during MSG welding of a rotating workpiece. As an example, the upper figure shows the desired torch orientation for usual welding speeds. This orientation depends on parameters like workpiece diameter and thickness, groove shape, melting rate, and welding speed. The lower figure illustrates variations of torch orientation on seam formation. A torch orientation should be chosen in such a way that a solidification of the melt pool takes place in 12 o'clock position, i.e. the weld pool does not flow in front or behind of the arc. Both may cause lack of fusion.

In contrast to faulty fusion, pores in the weld metal due to their globular shape are less critical, provided that their size does not exceed a certain value. Secondly, they must occur isolated and keep a minimum distance from each other. There are two possible mechanisms to develop cavities in the weld metal: the mechanical and the metallurgical pore formation. Figure 9.9 lists causes of a mechanical pore formation as well as possibilities to avoid them. To over-weld a cavity (lack

gases / gas developers	causes	avoidance
air	air in weld gap	increase weld gap area, use butt welds instead of fillet or overlap welds
water	humidity in weld gap, possibly chemically bonded in rust untight torch	remove humidity by preheating, remove rust layers, use butt welds instead of fillet or overlap welds periodic tightness check
grease residues	pollution or applied grease layers in the weld gap for lubrication purposes and/or avoidance of corrosion	eliminate grease through solvents, increase weld gap area, use butt welds instead of fillet or overlap welds
metals e.g. tin, zinc, etc.	too thick layers, too narrow gap, too high pressure	keep recommended layer thickness, remove metal coatings, increase weld gap area, use butt welds instead of fillet or overlap welds
pigments, solvents and bonding agents of paint	paints, e.g. manuacturing coatings in the weld gap	select favourable paint material (examination to DVS 0501), keep prescribed layer thickness, remove eventually too thick layers, ensure good degassing conditions in the gap, where possible, use butt welds instead of fillet or overlap welds

br-er-09-09.cdr © ISF 2005

aachen ISF

Mechanical Pore Formation

Figure 9.9

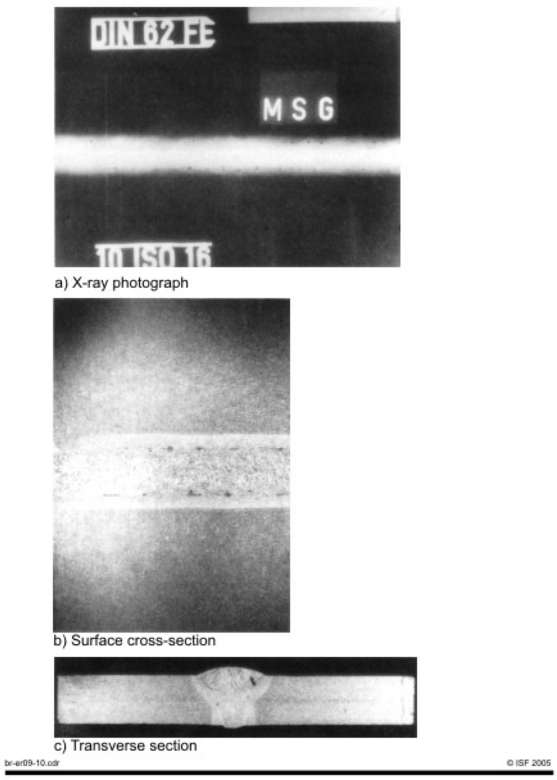

aachen ISF Mechanical Pore Formation

Figure 9.10

gas/gas developing material	causes	avoidance
air -nitrogen -hydrogen	**too low shielding gas flow through:**	
	too low setting	correct settings
	leaking lines	search and eliminate leaks
	too small capillary bore hole	correct combination capillary - pressure regulator
	too low supply pressure for pressure regulator	Pressure of bottles or lines must meet the required supply pressure of the pressure regulator
	insufficient gas shield through:	
	open windows, doors, fans etc.	protect welding point from draught
	insufficient gas flow at start and at completion of welding	suitable gas pre- and post-flow time
	too large gas nozzle distance	reduce distance
	excentric wire stick-out	straighten wire electrode, center contact tube
	false gas nozzle shape	select proper gas nozzle shape for joint type
	false gas nozzle position (with decentralised gas supply)	position gas nozzel behind torch - if possible
	turbulences through:	
	to high shielding gas flow	reduce gas flow
	spatters on gas nozzle or contact tube	clean gas nozzle and contact tube
	irregular arc	eliminate wire feed disturbances, increase voltage, if wire electrode splutters, ensure good current transition in contact tube, correct earth connection, remove slag of previously welded layers
	thermal current - possibly increased by chimmney effects with one-sided welding	weld on backing or with root forming gas
	too high weld pool temperature	reduce weld pool size
	too high work piece temperature	reduce preheat or interpass temperature
	injection effects	reduce torch inclination, tighten leaks in gas line, avoid visible gas nozzle slots
water	leaking torch (with water-cooled types)	search and eliminate leaks, dry wire feed hose after ingress of water
carbonmonoxide	remelting of seggregation zones	reduce penetration by decreasing arc power or increasing welding speed
	remelting of rust or scale	clean welding area before welding

br-er09-11.cdr © ISF 2002

aachen ISF Metallurgical Pore Formation

Figure 9.11

of fusion, gaps, overlaps etc.) of a previous layer can be regarded as a typical case of a mechanical pore formation.

The welding heat during welding causes a strong expansion of the gasses contained in the cavity and consequently a development of a gas bubble in the liquid weld metal. If the solidification is carried out so fast that this gas bubble cannot raise to the surface of the weld pool, the pore will be caught in the weld metal.

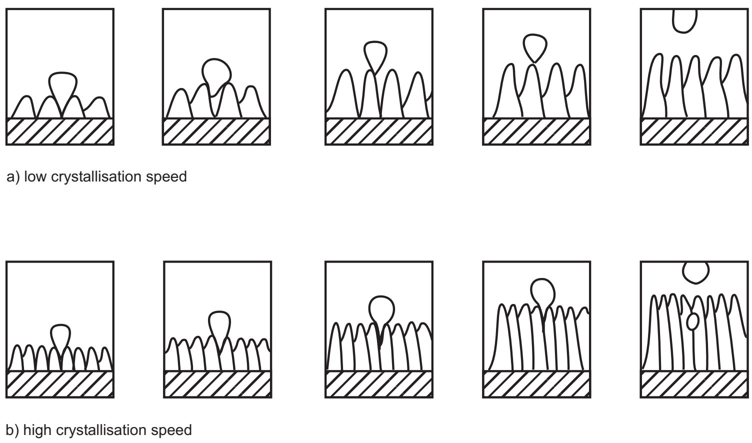

br-er-09-12.cdr © ISF 2002

aachen ISF Growth and Brake Away of Gas Cavities at the Phase Border

Figure 9.12

Figure 9.10 shows a X-ray photograph of a pore which developed in this way, as well as a surface and a transverse section. This pore formation shows its typical pore position at the edge of the joint and at the fusion line of the top layer.

Figure 9.11 summarises causes of and measures to avoid a metallurgical pore formation. Reason of this pore formation is the considerably increased solubility of the molten metal compared with the solid state.

During solidification, the transition of liquid to solid condition causes a leapwise reduction of gas solubility of the steel. As a result, solved gasses are driven out of the crystal and are enriched as a gas bubble ahead of the solidification front. With a slow growth of the crystallisation front, the bubbles have enough time to raise to the surface of the weld pool, Figure 9.12 upper part. Pores will not be developed. However, a higher solidification speed may lead to a case where gas bubbles are passed by the crystallisation front and are trapped as pores in the weld metal, lower part of the figure.

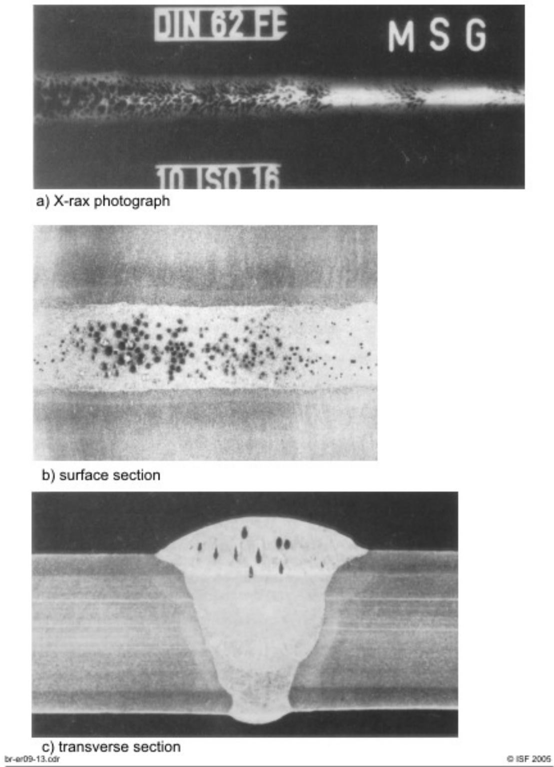

Metallurgical Pore Formation

Figure 9.13

Figure 9.13 shows a X-ray photograph, a surface and a transverse section of a seam with metallurgical pores. The evenly distributed pores across the seam and the accumulation of pores in the upper part of the seam (transverse section) are typical.

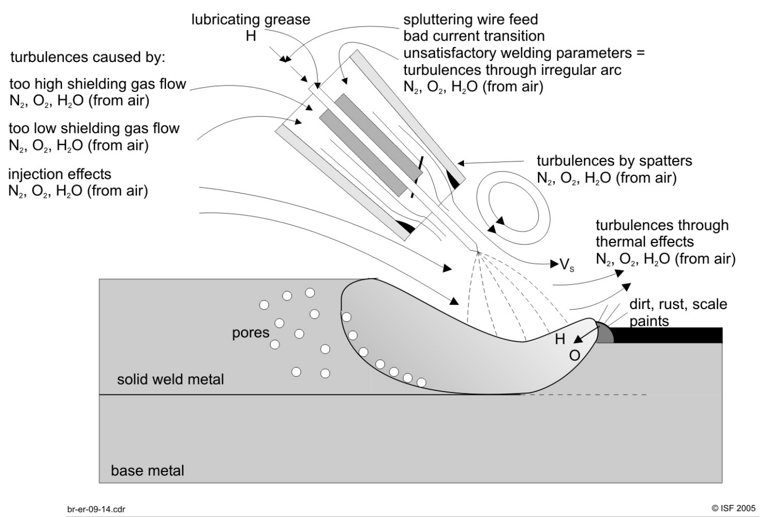

Possible Gas-Pick-up
During Gas Metal Arc Welding

Figure 9.14

Figure 9.14 shows the ways of ingress of gasses into the weld pool as an example during MAG welding. A pore formation is mainly caused by hydrogen and nitrogen. Oxygen is bonded in a harmless way when using universal electrodes which are alloyed with Si and Mn. Figure 9.15 classifies cracks to DIN 8524, part 3. In contrast to part 1 and 2 of this standard, are cracks not only classified by their appearance, but also by their development.

Classification number	Description	Explanation
100	Riss (1) crack fissure	limited material separation of mostly 2-dimensional shape (see DIN 8524 Sheet 1 Part 2)
Classification to crack size (2)		
100 1	Mikroriss micro-crack micro-fissure	crack, only visible under a magnification of more than factor 6
100 2	Makroriss macro-crack macro-fissure	crack, visible with normal eye (reference distance 250 mm) or under a magnification up to a factor of 6
Classification to crack propagation (3)		
100 01	interkristalliner Riss (Korngrenzenriss) intergranular crack (intercrystalline crack) fissure intergranulaire (fissure entre grains)	propagates along crystallite borders
100 02	transkristallinter Riss transgranular crack (transcrystalline crack) fissure transgranulaire	propagates through crystallites
100 03	inter- und transkristalliner Riss (i-t-Riss) intergranular and transgranular crack (i-t-crack) fissure inter- et transgranulaire (fissure-i-t)	propagates inter- and transgranular
Classification to conditions and causes of crack development		
100 0010	Heißriss (4) hot crack fissure à chaud	develops through a low-melting phase while it is liquid
100 0011	Erstarrungsriss solidification crack (crater crack) fissure de solidification	develops during solidification of the weld pool
100 0012	Aufschmelzungsriss liquation crack fissure de fusion	only the low-melting phase was molten, e.g. at a grain boundary
100 0020	Kaltriss cold crack fissure à froid	develops in solid condition of the material by exceeding ist deformation stress limit
100 0021	Sprödriss ductility-dip crack (brittle crack) fissure déclencée à l'état de basse tenacité	develops when the material passes a temperature-depending ductility minimum
100 0022	Schrumpfriss shrinkage crack fissure de retait	develops through impeded shrinking: structure components of low deformability or low strength favour ist formation
100 0023	Wasserstoffriss hydrogen induced crack (delayed crack) fissure induite par hydrogène	develops through an increase of the residual stress condition: hydrogen precipitates which cannot effuse out of the material due to microstructure changes
100 0024	Aufhärtungsriss age-hardening crack fissure par suite de durcissement	develops through microstructure changes: resulting volume changes cause stresses
100 0025	Kerbriss toe-crack fissure par entaille	develops in areas of high tension concentration (geometrical kerf) and simultaneously present metallurgical notch
100 0026	Alterungsriss ageing induced crack (nitogen diffusion crack) fissure par suite de vieillissement	develops through ageing processes
100 0027	Ausscheidungsriss precipition induced crack fissure par suite de durcissement structural	develops through precipitation of brittle phases during welding or post-weld heat treatment
100 0028	Lamellenriss lamellar tearing fissuration lamellaire	develops through tearing of parallel segregation zones with streched non-metallic inclusions when the workpiece is charged in thickness direction

(1) If crack surfaces do not tear, one spreacks of hairline cracking
(2) A method to identify a crack may be a non-destructive test procedure
(3) Intergranular and transgranular crack propagation can be marked with additional letters i and t, e.g. 1001
(4) If the low-melting phase is metallic, then it will be called solder crack (crack caused by low fusion point)

br-er09-15.cdr

aachen ISF

Classification of Cracks to DIN 8524 Part 3

Figure 9.15

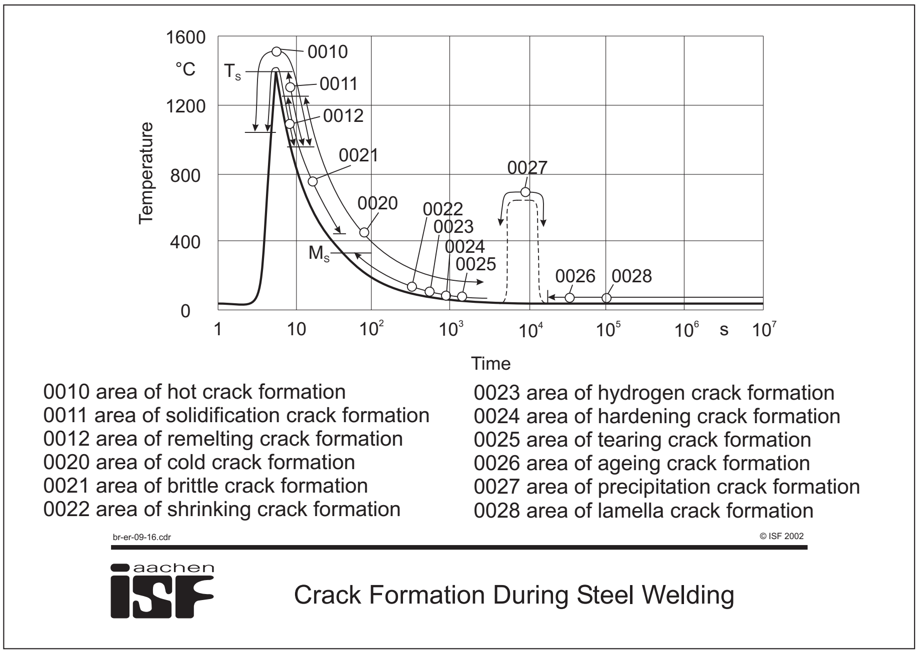

Figure 9.16

Figure 9.16 allocates cracks according to their appearance during the welding heat cycle. Principally there is a distinction between the group 0010 (hot cracks) and 0020 (cold cracks).

A model of remelting development and solidification cracks is shown in Figure 9.17. The upper part illustrates solidification conditions in a simple case of a binary system, under the provision that a complete concentration balance takes place in the melt ahead of the solidification front, but no diffusion takes place in the crystalline solid. When a melt of a composition C_0 cools down, a crystalline solid is formed when the liquidus line is reached. Its concentration can be taken from the solidus line. In the course of the ongoing solidification, the rest of molten metal is enriched with alloy elements in accordance with the liquidus line. As defined in the beginning, no diffusion of alloy elements in the already solidified crystal takes place, thus the crystals are enriched with alloy elements much slower than in a case of the binary system (lower line).

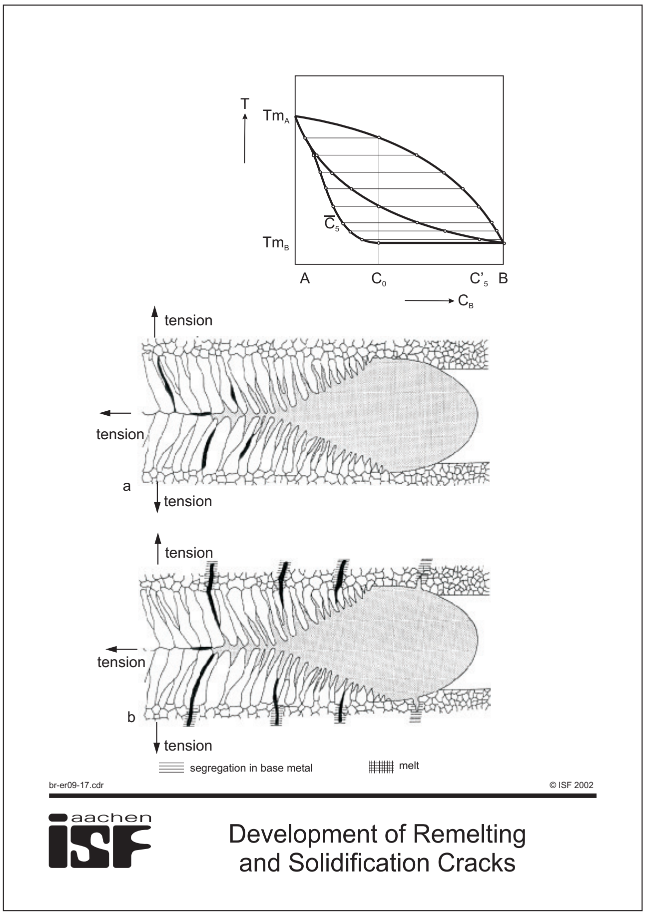

Figure 9.17

As a result, the concentration of the melt exceeds the maximum equilibrium concentration (C_5), forming at the end of solidification a very much enriched crystalline solid, whose melting point is considerably lower when compared with the firstly developed crystalline solid. Such concentration differences between first and last solidified crystals are called segregations. This model of segregation development is very much simplified, but it is sufficient to understand the mechanism of hot crack formation. The middle part of the figure shows the formation of solidification cracks. Due to the segregation effects described above, the melt between the crystalline solids at the end of solidification has a considerably decreased solidus temperature. As indicated by the black areas, rests of liquid may be trapped by dendrites. If tensile stresses exist (shrinking stress of the welded joint), the liquid areas are not yet able to transfer forces and open up.

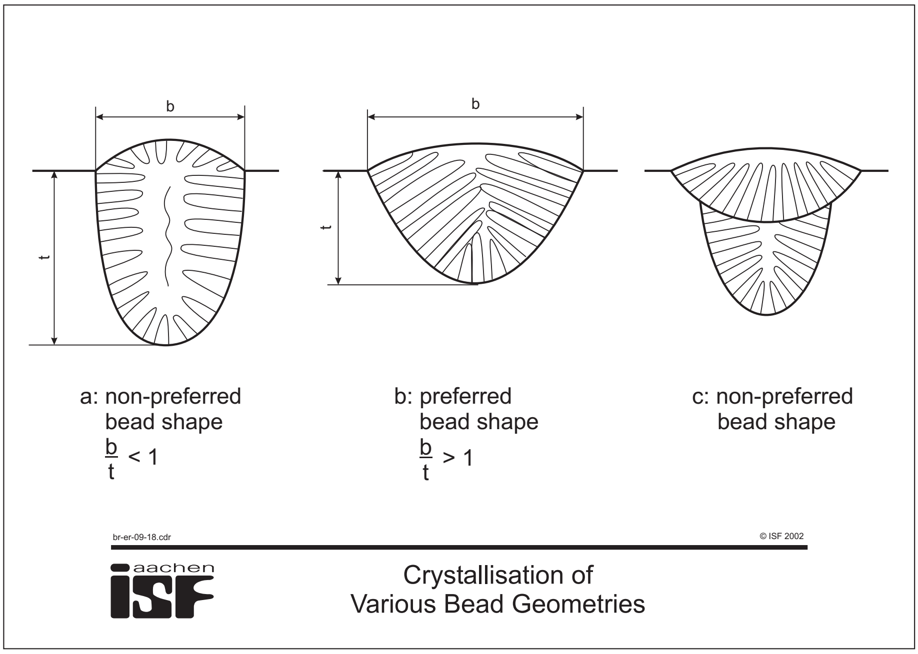

Figure 9.18

The lower part of the figure shows the development of remelting cracks. If the base material to be welded contains already some segregations whose melting point is lower than that of the rest of the base metal, then these zones will melt during welding, and the rest of the material remains solid (black areas). If the joint is exposed to tensile stress during solidification, then these areas open up (see above) and cracks occur. A hot cracking tendency of a steel is above all promoted by sulphur and phosphorus, because these elements form with iron very

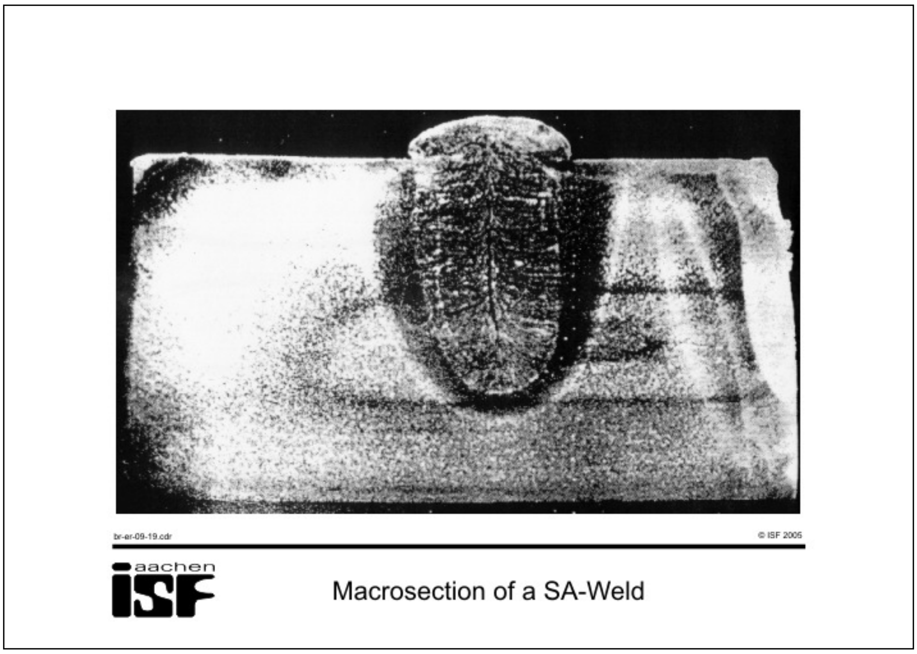

Figure 9.19

low melting phases (eutectic point Fe-S at 988°C) and these elements segregate intensely. In addition, hot crack tendency increases with increasing melt interval.

As shown in Figure 9.18, also the geometry of the groove is important for hot crack tendency. With narrow, deep grooves a crystallisation takes place of all sides of the bead, entrapping the remaining melt in the bead centre. With the occurrence of shrinking stresses, hot cracks may develop. In the case of flat beads as shown in the middle part of

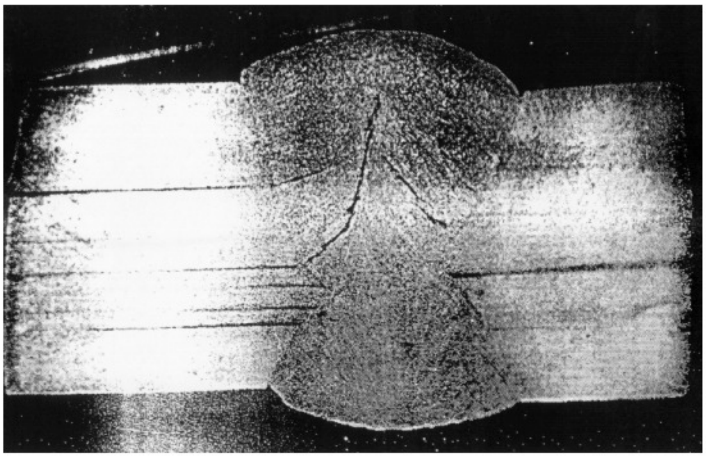

Macrosection of a SA-Weld

Figure 9.20

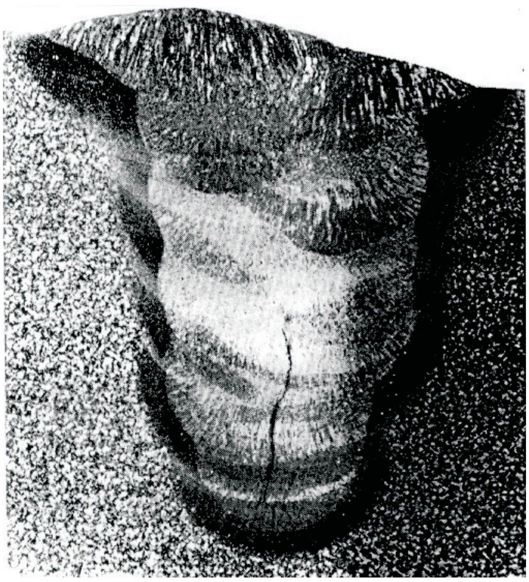

Macrosection of a SA-Weld

Figure 9.21

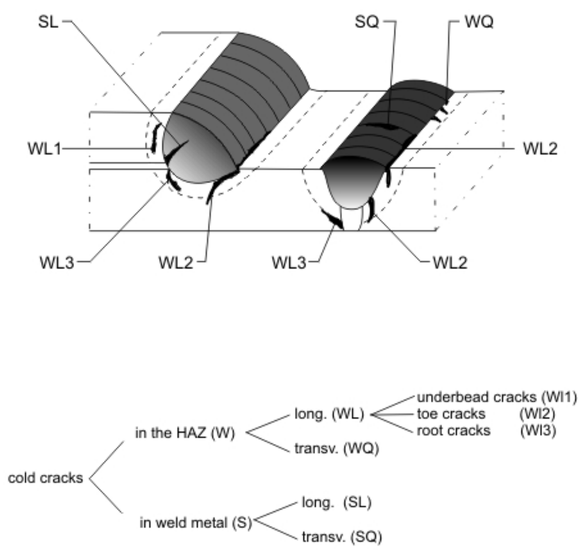

Classification of Cold Cracks

Figure 9.22

the figure, the remaining melt solidifies at the surface of the bead. The melt cannot be trapped, hot cracking is not possible. The case in figure c shows no advantage, because a remelting crack may occur in the centre (segregation zone) of the first layer during welding the second layer.

The example of a hot crack in the middle of a SA weld is shown in Figure 9.19. This crack developed due to the unsuitable groove geometry.

Figure 9.20 shows an example of a remelting crack which started to develop in a segregation zone of the base metal and spread up to the bead centre.

The section shown in Figure 9.21 is similar to case c in Figure 9.18. One can clearly see that an existing crack develops through the following layers during over-welding.

Figure 9.22 classifies cold cracks depending on their position in the weld metal area. Such a classification does not provide an explanation for the origin of the cracks.

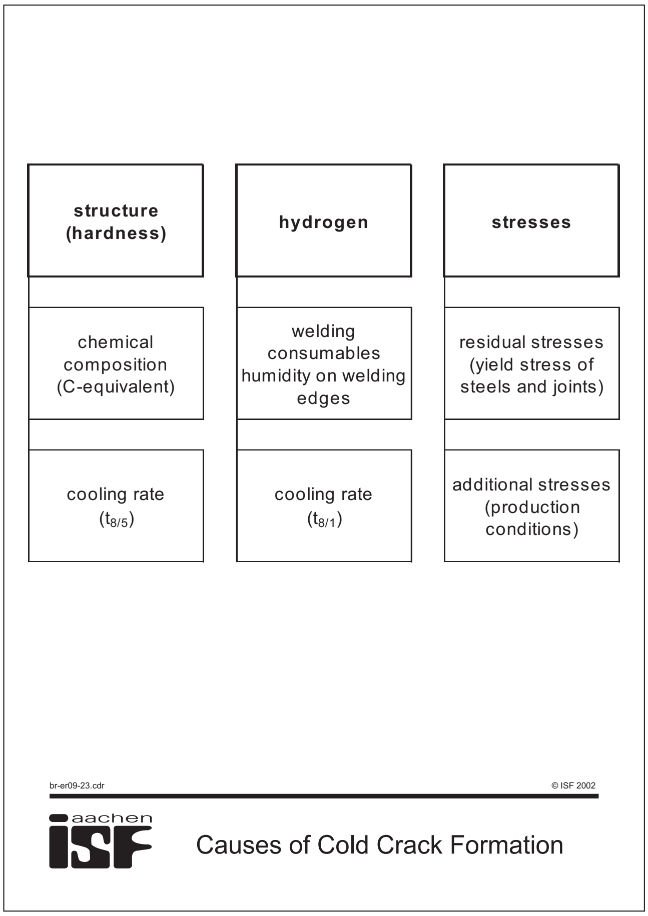

Figure 9.23

Figure 9.23 shows a summary of the three main causes of cold crack formation and their main influences. As explained in previous chapters, the resulting welding microstructure depends on both, the composition of base and filler materials and of the cooling speed of the joint. An unsatisfactory structure composition promotes very much the formation of cold cracks (hardening by martensite).

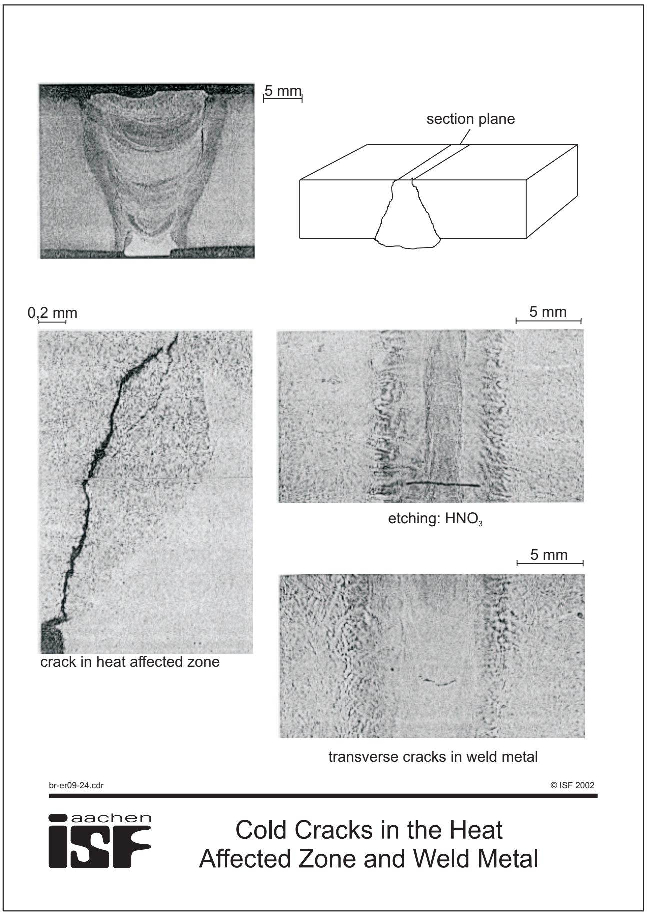

Figure 9.24

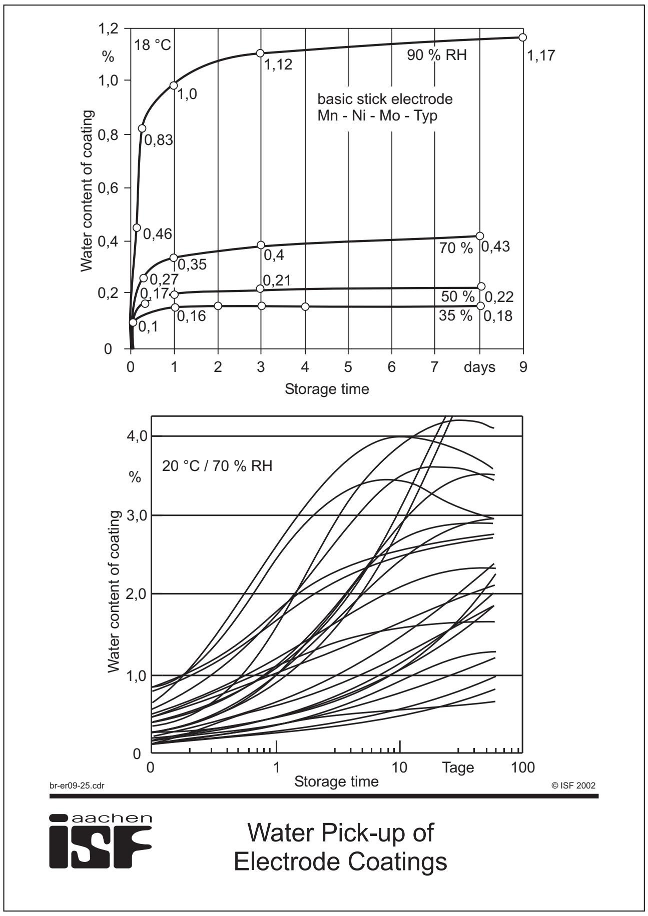

Figure 9.25

Another cause for increased cold crack susceptibility is a higher hydrogen content. The hydrogen content is very much influenced by the condition of the welding filler material (humidity of electrodes or flux, lubricating grease on welding wire etc.) and by humidity on the groove edges.

The cooling speed is also important because it determines the remaining time for hydrogen effusion out of the bead, respectively how much hydrogen remains in the weld. A measure is $t_{8/1}$ because only below 100℃ a hydrogen effusion stops.

A crack initiation is effected by stresses. Depending on material condition and the two already mentioned influencing factors, even residual stresses in the workpiece may actuate a crack. Or a crack occurs only when superimpose of residual stresses on outer stress.

Figure 9.24 shows typical cold cracks in a workpiece. An increased hydrogen content in the weld metal leads to an increased cold crack tendency. Mechanisms of hydrogen cracking were not completely understood until today. However, a spontaneous occurrence is typical of hydrogen cracking. Such cracks do not appear directly after welding but hours or even days after cooling. The weld metal hydrogen content depends on humidity of the electrode coating (manual metal arc welding) and of flux (submerged arc welding).

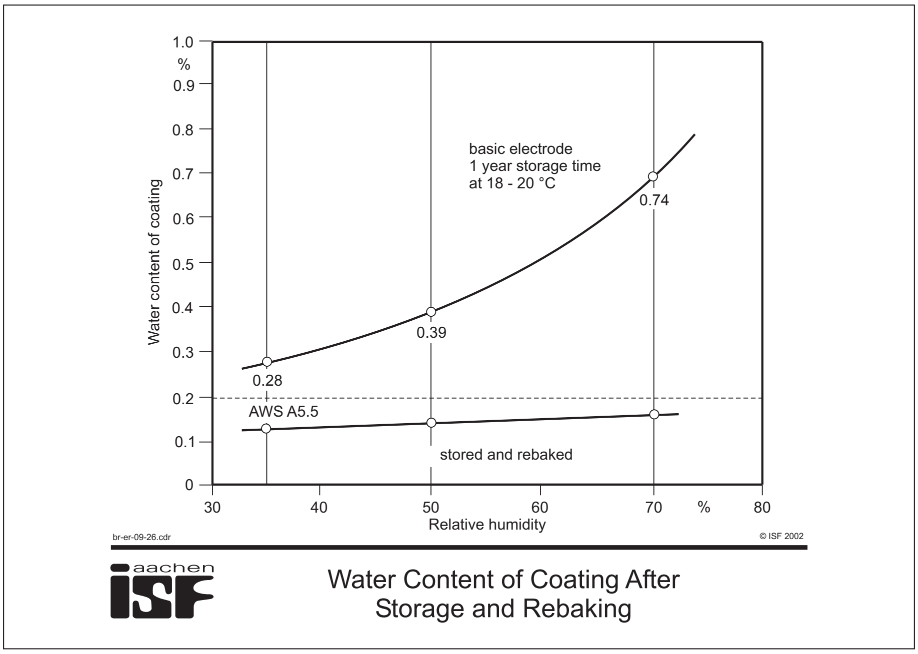

Figure 9.26

Figure 9.25 shows that the moisture pick-up of an electrode coating greatly depends on ambient conditions and on the type of electrode. The upper picture shows that during storage of an electrode type the water content of the coating depends on air humidity. The water content of the coating of this electrode type advances to a maximum value with time. The lower picture shows that this behaviour does not apply to all electrode types. The characteristics of 25 welding electrodes stored under identical conditions are plotted here. It can clearly be seen that a behaviour as shown in the upper picture applies only to some electrode types, but basically a very different behaviour in connection with storage can be noticed.

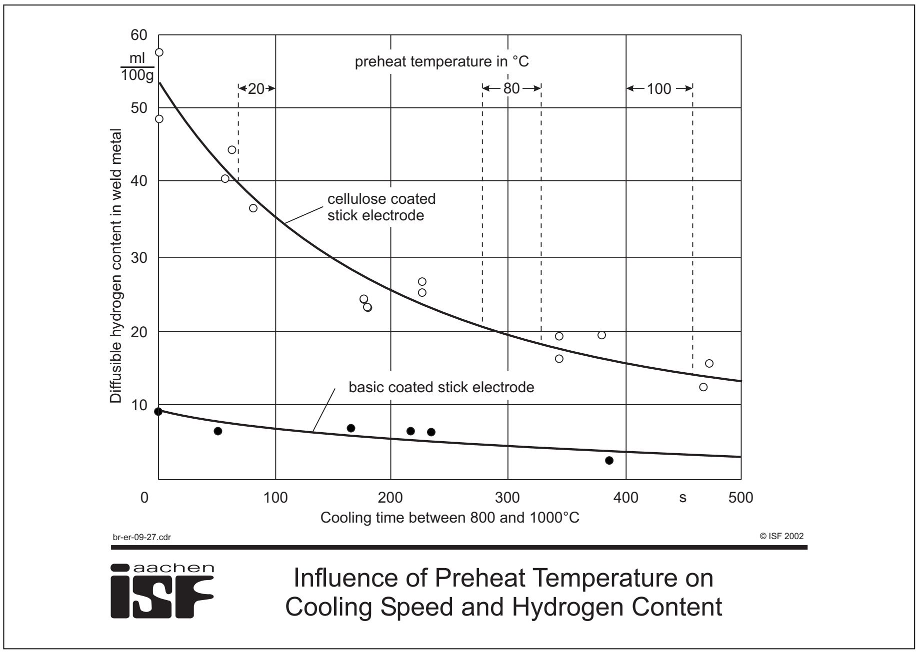

Figure 9.27

In practice, such constant storage conditions are not to be found, this is the reason why electrodes are backed before welding to limit the water content of the coating. Figure 9.26 shows the effects of this measure. The upper curve shows the water content of the coating of electrodes which were stored at constant air humidity before rebaking. Humidity values after rebaking are plotted in the lower curve. It can be seen that even electrodes stored under very damp conditions can be rebaked to reach acceptable values of water content in the coating.

Figure 9.27 shows the influence of cooling speed and also the preheat temperature on hydrogen content of the weld metal. The values of a high hygroscopic cellulose-coated electrode are considerably worse than of a basic-coated one, however both show the same tendency:

increased cooling speed leads to a raise of diffusible hydrogen content in weld metal. Reason is that hydrogen can still effuse all the way down to room temperature, but diffusion speed increases sharply with temperature. The longer the steel takes to cool, the more time is available for hydrogen to effuse out of the weld metal even in higher quantities.

Designation	Hydrogen content ml/100 g deposited weld metal	
high	>15	
medium	≤ 15 and > 10	in ISO 2560 classified as H-controlled electrodes
low	≤ 10 and > 5	
very low	≤ 5	

br-er-09-28.cdr © ISF 2002

Assessment of Diffusible Hydrogen During Manual Metal Arc Welding

Figure 9.28

The table in Figure 9.28 shows an assessment of the quantity of diffusible hydrogen in weld metal according to DIN 8529.

Based on this assessment, a classification of weld metal to DIN 32522 into groups depending on hydrogen is carried out, Figure 9.29.

Abbreviation	Hydrogen content ml/100 g deposited weld metal (max.)
HP 5	5
HP 7	7
HP 10	10
HP 15	15

br-er-09-29.cdr © ISF 2002 H_2-Bestimmung nach DIN 8572,2

Diffusible Hydrogen of Weld Metal to DIN 32522

Figure 9.29

A cold crack development can be followed-up by means of sound emission measurement. Figure 9.30 represents the result of such a measurement of a welded component. A solid-borne sound microphone is fixed to a component which measures the sound pulses generated by crack development. The intensity of the pulses provides a qualitative assessment of the crack size. The observation is carried out without applying an external tension, i.e. cracks develop only caused by the internal residual stress condition. Figure 9.32 shows that most cracks occur relatively short after welding. At first this is due to the cooling process. However, after completed cooling a multitude of developing sounds can be registered. It is remarkable that the intensity of late occurring pulses is especially high. This behaviour is typical for hydrogen induced crack formation.

Figure 9.31 shows a characteristic occurrence of lamellar cracks (also called lamellar tearing). This crack type occurs typically during stressing a plate across its thickness (perpen-

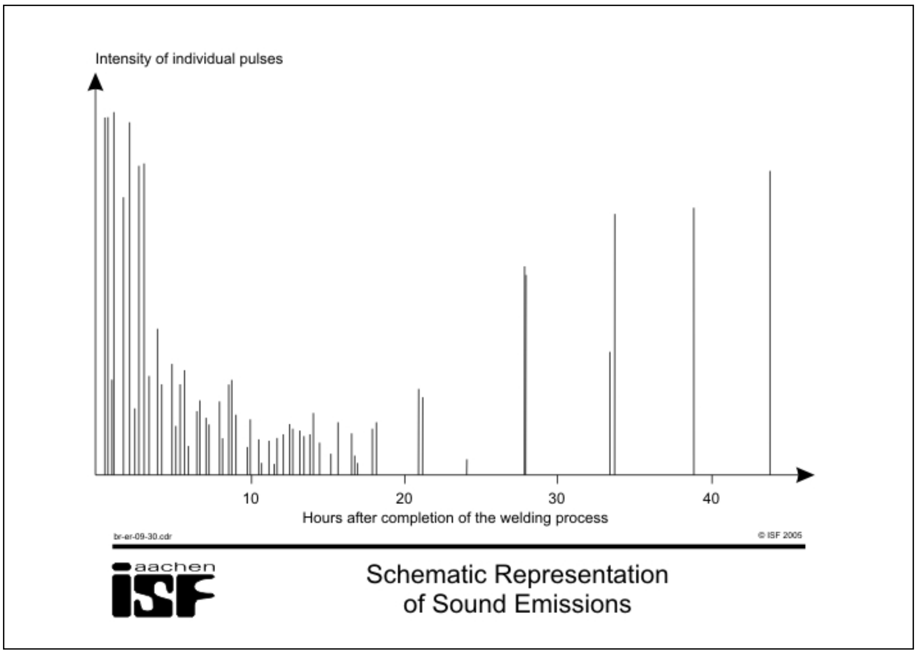

Figure 9.30

dicular to rolling direction). The upper picture shows joint types which are very much at risk to formation of such cracks. The two lower pictures show the cause of that crack formation. During steel production, a formation of segregation cannot be avoided due to the casting process. With following production steps, such segregations are stretched in the rolling direction. Zones enriched and depleted of alloy elements are now close together.

These concentration differences influence the transformation behaviour of the individual zones. During cooling, zones with enriched alloy elements develop a different microstructure than depleted zones. This effect which can be well recognised in Figure 9.31, is called structure banding. In practice, this formation can be hardly avoided. Banding in plates is the reason for worst mechanical properties perpendicular to rolling direction. This is caused by a different mechanical behaviour of different microstructures.

When stressing lengthwise and transverse to rolling direction, the individual structure bands may support each other and a mean strength is provided.

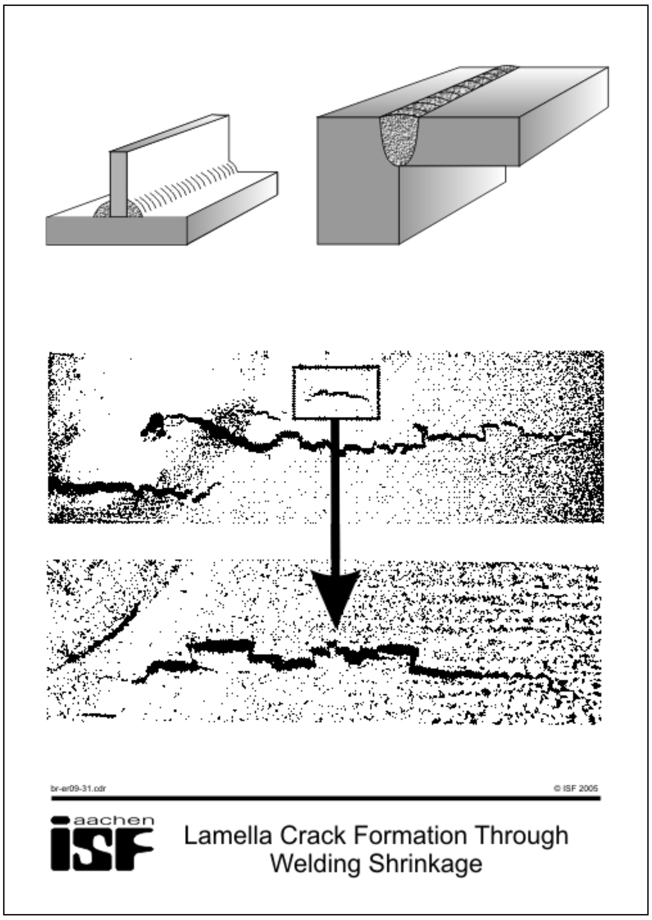

Figure 9.31

Such support cannot be obtained perpendicular to rolling direction, thus the strength of the workpiece is that of the weaker microstructure areas. Consequently, a lamellar crack propagates through weaker microstructure areas, and partly a jump into the next band takes place.

Figure 9.32 illustrates why such t-joints are particularly vulnerable. Depending on joint shape, these welds show to some extent a considerable shrinking. A welded construction which greatly impedes shrinking of this joint, may generate stresses perpendicular to the plane of magnitude above the tensile strength. This can cause lamellar tearing.

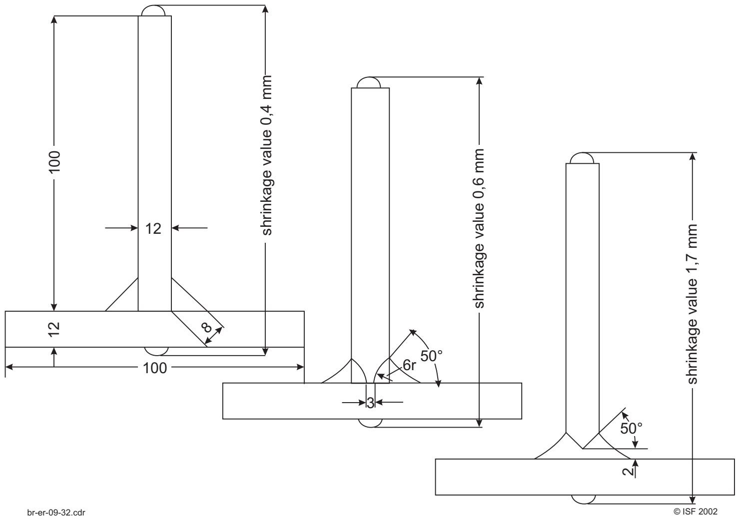

aachen ISF Shrinkage Values of T-Joints With Various Joint Shapes

Figure 9.32

Precipitation cracks occur mainly during stress relief heat treatment of welded components. They occur in the coarse grain zone close to fusion line. As this type of cracks occurs often during post weld heat treatment of cladded materials, is it also called undercladding crack, Figure 9.33.

Especially susceptible are steels which contain alloy elements with a precipitation hardening effect (carbide developer like Ti, Nb, V). During welding such steels, carbides are dissolved in an area close to the fusion line. During the following cooling, the carbide developers are not completely re-precipitated.

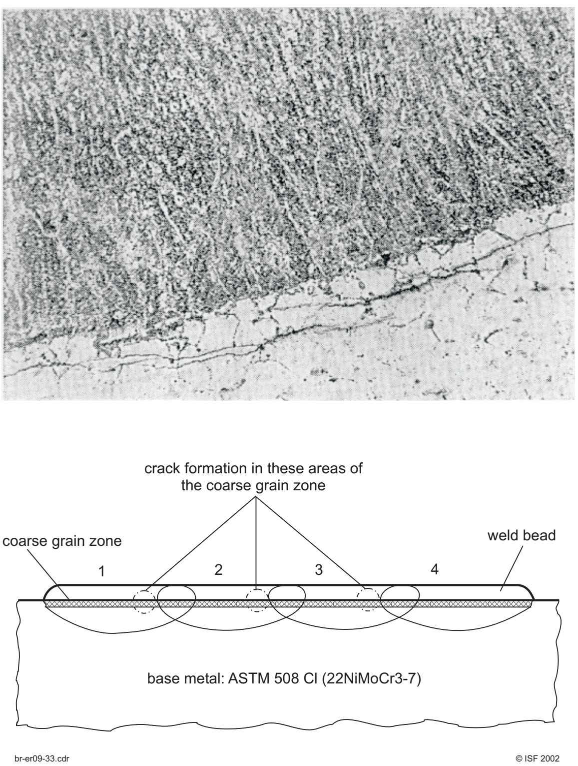

aachen ISF Undercladding Cracks

Figure 9.33

If a component in such a condition is stress relief heat treated, a re-precipitation of carbides takes place (see hot ageing, chapter 8). With this re-precipitation, precipitation-free zones may develop along grain boundaries, which have a considerably lower deformation stress limit compared with strengthened areas. Plastic deformations during stress relieving are carried out almost only in these areas, causing the cracks shown in Figure 9.33.